Directing-Group-Free Arene C(sp²)–H Amination using Bulky Aminium Radicals and DFT Analysis of Regioselectivity

Nicole Erin Behnke[1‡†], Young-Do Kwon[1‡], Michael T. Davenport[2], Daniel H. Ess[2*], and László Kürti[1*]

[1]Department of Chemistry, Rice University, Houston, Texas 77030, USA; [2]Department of Chemistry and Biochemistry, Brigham Young University, Provo, Utah 84602, USA; E-mail: kurti.laszlo@rice.edu, dhe@chem.byu.edu

Supporting Information Placeholder

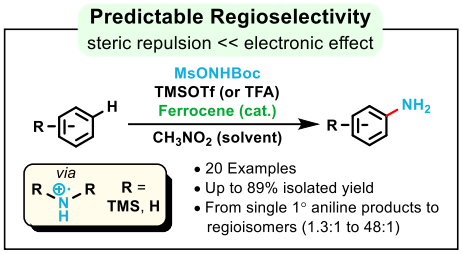

ABSTRACT: A hydroxylamine-derived electrophilic aminating reagent produces a transient and bulky aminium radical intermediate upon *in-situ* activation by either TMSOTf or TFA and a subsequent electron transfer from an iron(II)-catalyst. Density functional theory calculations were used to examine the regioselectivity of arene C–H amination reactions on diversely substituted arenes. The calculations suggest a simple charge-controlled regioselectivity model that enables prediction of the major C(sp²)–H amination product.

INTRODUCTION

Aromatic amines are ubiquitous structural motifs and important building blocks in the chemical industry.[1,2] Due to their frequent occurrence in biologically active molecules and consumer products, significant efforts have been dedicated to developing efficient methods for their expedient synthesis.[2] Well-developed and general strategies include the reduction of nitroarenes,[3] transition metal-catalyzed cross-coupling reactions (i.e., Buchwald–Hartwig, Chan–Lam–Evans, etc.),[4] and electrophilic amination of arylmetals and arylboronic acids.[5] More recently, C–H amination has received widespread attention as a powerful tool to access arylamines without pre-functionalization of the aromatic substrates.[6] Both types of C–H amination, directed and directing-group-free, operate with high atom and step economies when individual C–H bonds can be selectively transformed (Figure 1A). Directed, or guided, C–H amination relies on specially-designed functional groups serving as discrete directing groups to control the regioselectivity of C–N bond formation. Although directed C–H amination reactions can generally achieve excellent regioselectivity, the required installation and presence of a directing group is often undesirable, especially for target-oriented synthesis. On the other hand, directing-group-free C–H amination takes advantage of the innate steric and/or electronic properties of the substrates to induce regiocontrol. Unfortunately, directing-group-free approaches typically afford regioisomeric product mixtures, which ultimately lead to suboptimal yields and challenging purification.

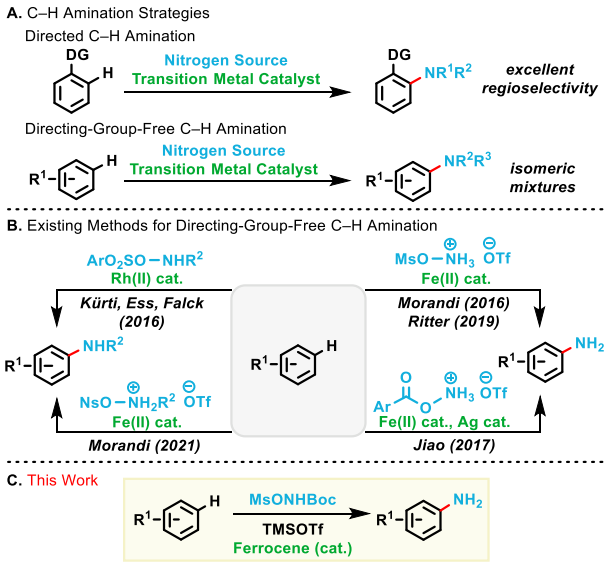

Figure 1. Transition Metal-Catalyzed Aromatic C–H amination.

In the past several years, a handful of directing-group-free arene C–H amination methods have been reported (Figure 1B). For the synthesis of secondary arylamines, Kürti and Falck reported the dirhodium-catalyzed intermolecular

C–H amination of electron-rich arenes with NH(alkyl)-*O*-(arylsulfonyl)-hydroxylamine aminating agents.[7] Similar *N*-alkyl aniline products can be generated via Fe-catalyzed C–H amination of substituted arenes using *O*-(arylsulfonyl)-hydroxylamine triflate salts.[8] Morandi[9] and Ritter[10] also reported directing-group-free C–H primary amination using acidified *O*-(alkylsulfonyl)-hydroxylamines and a Fe(II)-catalyst. Jiao and coworkers also demonstrated a Fe-catalyzed primary C–H amination with *O*-(aroyl)-hydroxylamine triflate salts.[11] Building upon these precedents, we proposed the use of *O*-(methanesulfonyl)-*N*-*tert*-butyloxycarbonyl hydroxylamine (MsONHBoc), a bench-stable aminating agent. In the presence of TMS-triflate and an electron transfer catalyst, this reagent would generate, *in-situ*, a bulky TMS-substituted aminium radical species that should be capable of performing regioselective arene C–H amination (Figure 1C). In this study, we demonstrate the versatility of MsONHBoc in conjunction with a wide variety of aromatic compounds for the production of corresponding anilines. To gain a deeper understanding, we employed density functional theory (DFT) calculations to investigate the energy landscape of amination and evaluate the influence of the bulky TMS groups. Surprisingly, our calculations revealed that the charge of the transition state, rather than steric factors, governs the regioselectivity, aligning with Ritter's earlier proposal.[12] Leveraging this finding, we developed a straightforward DFT thermodynamic calculation model that allows the prediction of the major primary aniline regioisomer in arene C–H amination reactions.

RESULTS AND DISCUSSION

The Fe^{2+} → Fe^{3+} redox system has been successfully employed in catalytic electron transfer processes for aromatic C–H amination.[8–11] We decided to use the well-defined and stable 1,1'-diacetylferrocene (Fc/Fc^{+}) platform to serve as our initial electron transfer catalyst. For the optimization of the reaction conditions, 2,4-dibromoanisole (**1**) was selected as the substrate – it was determined that two equivalents of the aminating agent and three equivalents of the TMS-triflate had to be used in nitromethane (CH_3NO_2) solvent in order to obtain the best results (see SI, Table S1). Thus, amination of arene **1** with MsONHBoc resulted in primary aromatic amines **2A** and **2B**, where the major and minor regioisomers were formed by C–H amination at the 5- and 6-positions, respectively.

Table 1. Optimization of Reaction Conditions for Fe-Catalyzed Directing-Group-Free C–H Amination of Arenes[a]

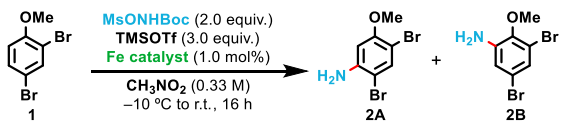

Entry	Fe catalyst	Yield (%)[b] **2A**	Yield (%)[b] **2B**
1	1,1'-diacetylferrocene	31	18
2[c]	1,1'-diacetylferrocene	12	9
3[d]	1,1'-diacetylferrocene	trace	trace
4	1,1'-dimethylferrocene	31	19
5	1,1'-dibromoferrocene	19	9
6	acetylferrocene	33	20
7	**ferrocene**	**45**	**27**

[a]Reaction scale: 0.50 mmol. [b]Isolated yields after purification. [c]TES-triflate instead of TMS-triflate. [d]TIPS-triflate instead of TMS-triflate.

Next, further screening was performed by evaluating a variety of electron transfer catalysts (i.e., unsubstituted as well as substituted ferrocenes) and trialkylsilyl-triflate additives (Table 1). Exchanging the TMS-triflate additive for TES-triflate (Table 1, entry 2) or TIPS-triflate (Table 1, entry 3) resulted in diminished product yields, presumably due to the decreased reactivity of the bulkier silyl triflate reagents. We found that unsubstituted ferrocene performed best by improving the isolated yield of major aniline isomer **2A** up to 45% (Table 1, entry 7). Overall, the optimized conditions include two equivalents of the aminating agent (MsONHBoc), three equivalents of TMS-triflate as an additive, 1.0 mol% of ferrocene as the catalyst, and nitromethane as the solvent at a temperature gradient of –10 °C to room temperature with overnight stirring.

Next, the substrate scope was explored under the optimized conditions (Table 2). The depicted yields correspond to the major product (i.e., indicated as *position A* on the aromatic ring) and the ratio of regioisomers was determined either via integrating the peaks of the crude NMR spectrum or via the isolated yields of the individual regioisomers after separating these via flash chromatography.

Table 2. Substrate Scope for the Fe-Catalyzed Directing-Group-Free C–H Amination of Arenes[a]

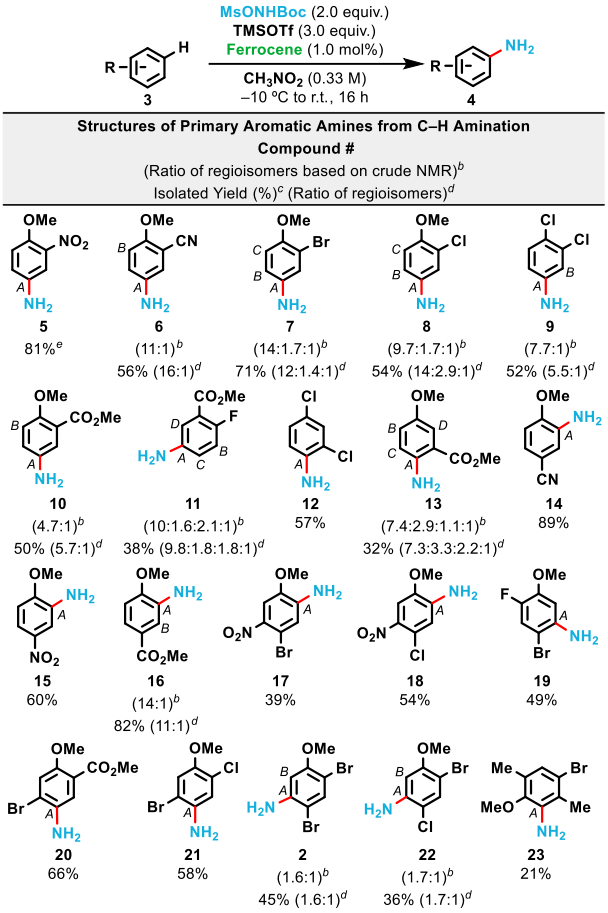

[a]Reaction scale: 0.50–1.0 mmol. [b]The ratio of regioisomers is based on crude NMR after basic work-up. [c]Isolated yield corresponding to the major isomer (indicated as *position A* on arenes). [d]The ratio of regioisomers is based on isolated yields. [e]78% isolated yield at the reaction scale of 3.3 mmol.

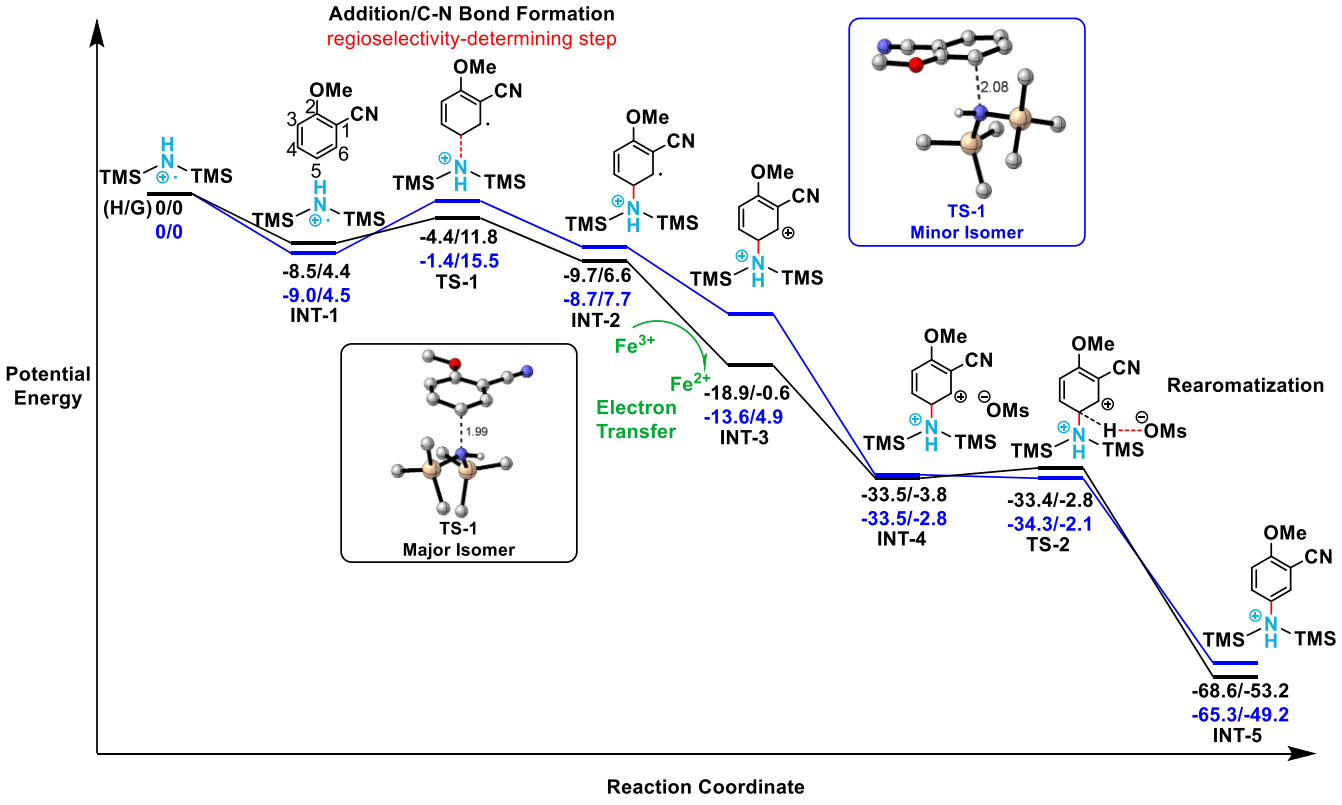

Figure 2. M06-2X energy landscape for reaction between $[(TMS)_2NH]^{\bullet+}$ radical cation and 2-methoxybenzonitrile. Black lines represent energies for the major regioisomer. Blue lines represent energies for the minor regioisomer. Enthalpies/Gibbs energies reported in kcal/mol. 3D Depiction of M06-2X optimized C-N transition state structures with bond distances (Å).

Starting with 1,2-disubstituted arenes, primary amines **5**–**11** were obtained in moderate to good isolated yields (i.e., up to 81%), with excellent selectivity between the major isomer at *position A* and the minor isomer(s) at the other position(s). A larger scale reaction (i.e., 3.3 mmol instead of the usual 0.50 mmol scale) for the preparation of primary amine **5** resulted in a 78% isolated yield, which is a comparable result with the reaction at 0.50 mmol scale. For 1,3-disubstituted arenes, primary aniline **12** was isolated as the exclusive isomer in 57% isolated yield, while product **13** (i.e., amino group at *position A*) was formed with moderate regioselectivity out of the four isolated regioisomeric products. For 1,4-disubstituted arenes, amines **14** and **15** were formed exclusively with isolated yields up to 89%, but amine **16** was formed with excellent regioselectivity of 14:1 and with a high yield of 82%. Tri-substituted arene substrates yielded primary anilines **2** and **17**–**22** in yields up to 66%. Depending on the substitution pattern (i.e., 1,2,4- or 1,3,4- or 1,2,5-) and the overall electronic properties of the substrates, either single primary aniline products (**17**–**21**) were formed or two-component isomeric product mixtures (**2** and **22**) were obtained. Finally, the reaction of a tetra-substituted arene provided primary aniline **23** as the sole product in 21% isolated yield.

It has previously been proposed that C–H amination in these catalytic reactions occurs through a reactive nitrogen-centered radical or radical cation.[8–11] To examine the proposed generation of an aminium-type species, we used M06-2X DFT calculations to examine reaction mechanisms and regioselectivity. M06-2X/6-31+G** calculations (see SI, Table S3 for comparison of other basis sets and functionals) with the SMD nitromethane continuum solvent model were carried out in Gaussian 16. CREST/x-TB was used to generate all transition-states and intermediate conformations followed by full DFT optimization. We assumed that TMS-triflate induces conversion of MsONHBoc to $[(TMS)_2NH(OMs)]^+$ cation and that ferrocene reduction can generate either a $[(TMS)NH]^{\bullet}$ radical or a $[(TMS)_2NH]^{\bullet+}$ radical cation. Because formation of the neutral $[(TMS)NH]^{\bullet}$ radical is endothermic by ~10 kcal/mol and the formation of $[(TMS)_2NH]^{\bullet+}$ radical cation is exothermic by >20 kcal/mol, we decided to use the latter as a model for reaction with arenes (i.e., C–H amination). While it is possible that this radical cation can be converted to $[(TMS)_2N]^{\bullet}$ radical, through the loss of a proton, this neutral radical is much less reactive towards arenes, and the barriers are higher for addition to arenes (See SI, Figure S1).

For 2-methoxybenzonitrile, that furnishes primary aniline product **6**, we examined a complete reaction coordinate profile with the $[(TMS)_2NH]^{\bullet+}$ radical cation (Figure 2). Prior to bond-formation, there is a weak association/charge-transfer complex (**INT-1**) between the arene and cation radical amine, but on the Gibbs surface the structure is endergonic. This complex results in the activation enthalpy for C–N bond formation being slightly lower than separated reactants. Relative to **INT-1**, the C–N bond forming addition transition state, **TS-1**, at the 5-position requires an activation enthalpy ($\Delta H^{\ddagger}$) of 4.1 kcal/mol and Gibbs barrier ($\Delta G^{\ddagger}$) of 7.4 kcal/mol. The resulting dearomatized cation radical intermediate (**INT-2**) is slightly more endothermic than the initial charge-transfer complex. Electron transfer (ET) from **INT-2** to ferrocenium cation is exothermic by 3 kcal/mol. Marcus-theory analysis suggests that there is only a small amount of reorganization energy required to promote ET between **INT-2** and ferrocenium and therefore the barrier for this process is close to the thermodynamic energy change (see SI, Figure S2). After ET, there is a very small barrier (<2 kcal/mol) and highly exothermic reaction steps (>30 kcal/mol) for rearomatization. We modeled this rearomatization using the weakest base possible in the reaction solution, the $^-$OMs anion, which is **TS-2**. While we propose ET at **INT-2**, we cannot rule out deprotonation (either at the aromatic ring or nitrogen) prior to ET (See SI, Scheme S1).

Based on the reaction energy landscape between $[(TMS)_2NH]^{\bullet+}$ radical cation and 2-methoxybenzonitrile, the regioselectivity-determining step is the C–N bond formation since after this step there are fast and irreversible steps with very low barriers for ET and rearomatization. Consistent with experiments, the calculated $\Delta\Delta H^{\ddagger}$ between addition at the 5-position and the 3-position of 2-methoxybenzonitrile is 3.0 kcal/mol ($\Delta\Delta G^{\ddagger}$ = 3.7 kcal/mol). Using DLPNO-CCSD(T) the **TS-1** $\Delta\Delta H^{\ddagger}$ value between the 5-position and 3-position is also 3.0 kcal/mol. These wavefunction and DFT energies are consistent with the experimental 16:1 ratio. Inspection of the **TS-1** geometries for positions 3 and 5 shows a difference in the C–N bond length. In the major 5-position product transition state, the C–N bond is more advanced with a distance of 1.99 Å while the minor 3-position transition state has a longer distance of 2.08 Å.

To examine if indeed the C–N bond-forming step determines regioselectivity, we calculated **TS-1** for the major and minor regioisomers of eight different arenes shown in Table 2 that lead to aryl amine products **2**, **6**, **7**, **9**, **12**, **14**, **15**, and **16**. These eight arenes were selected because they range in selectivity from 1.7:1 to 14:1 and all the way to the exclusive generation of a single product (e.g. **12**, **14**, and **15**). Based on the lowest-energy transition-state structures for each regioisomer, seven out of these eight arenes examined showed M06-2X calculated regioselectivity consistent with experiment. However, there was only qualitative correlation between calculated $\Delta\Delta G^{\ddagger}$ values and the experimental product ratios. This is perhaps not unexpected since the experimental ratio is after reaction workup and likely not a kinetic ratio. As an example, for 4-methoxybenzonitrile (primary aniline product **14**), C–N bond formation at the 3-position has a barrier of 4.6 kcal/mol lower in energy (based on a Boltzmann averaged ensemble of transition-state conformations) than the 2-position, which is consistent with a single product formed. Similarly, for arenes that result in aryl amine products **6**, **7**, and **12**, all of which have relatively high or exclusive regioselectivities, the Boltzmann averaged energy difference between transition state conformations was equal to or greater than 2.8 kcal/mol. Perhaps expected

due to the relatively low 1.7:1 selectivity for 2,4-dibromo-1-methoxybenzene that gives aryl amine product **2**, M06-2X transition states incorrectly predict the 6-position addition to have a 0.7 kcal/mol lower Gibbs barrier than the 5-position addition. However, from a DFT calculation perspective, this energy difference is within the error of the calculation method and is larger than differences that occur when changing basis sets and density functionals (see SI, Table S3).

Because $[(TMS)_2NH]^{\bullet+}$ radical cation contains two sterically bulky TMS groups, we initially assumed that the regioselectivity for C–N bond formation was controlled by repulsive interactions with substituent groups of arenes. Therefore, we calculated the relative energies of **TS-1** with $[(SiH_3)_2NH]^{\bullet+}$, $[(CH_3)_2NH]^{\bullet+}$, and $[NH_3]^{\bullet+}$ radical cations. We expected that this series of modified radical cations would yield a decrease in the relative $\Delta\Delta G^{\ddagger}$ values. *Surprisingly, the opposite was found*: $[(CH_3)_2NH]^{\bullet+}$ and $[NH_3]^{\bullet+}$ radical cations gave $\Delta\Delta G^{\ddagger}$ values of 4.2 and 5.7 kcal/mol, respectively, which are both larger than the 3.7 kcal/mol value for the $[(TMS)_2NH]^{\bullet+}$ radical cation. *This suggests that regioselectivity is not governed by a repulsive steric interaction, but rather by an electronic effect.* This viewpoint is consistent with Ritter's previous proposal of charge-transfer type control of selectivity.[12]

To have more insight about an electronic effect being the governing factor on the regioselectivity, additional aromatic C–H aminations with $[NH_3]^{\bullet+}$ radical cation were performed. 2-Methoxybenzonitrile was chosen as the substrate, and TFA was selected as the additive which led to the formation of a protonated aminyl radical. Initially, very strong organic acids (i.e., triflic acid and methanesulfonic acid) were used, but the isolated yield for primary aniline **6** was dramatically decreased compared to the previous reaction conditions in which TMS-triflate was used (See SI, Table S2). We assumed that such strong acids led to the undesired decomposition of reaction components. Eventually, it was found that the C–H amination in the presence of TFA provides comparable isolated yields with the original reaction conditions that used TMS-triflate as the additive. Although TFA and TMS-triflate generate different counter anions, we assumed that there would be very marginal or no effect on arene C–H aminations based on the M06-2X energy landscape in Figure 2. For 10 substrates (**2**, **6**–**11**, **13**, **16**, and **22**), the amination was repeated under the original reaction condition with a single modification that employed TFA instead of TMS-trilate as the additive (Table 3).

Table 3. Aromatic C–H Amination with Protonated Aminyl Radical[a]

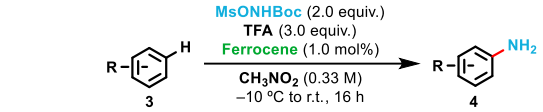

Structures of Primary Aromatic Amines from C–H Amination
Compound #
(Ratio of regioisomers based on crude NMR)[b]
Isolated Yield (%)[c] (Ratio of regioisomers)[d]

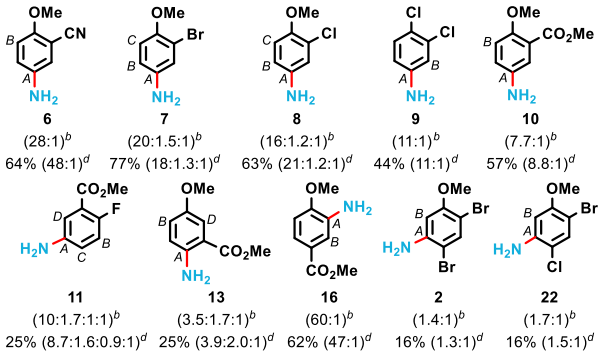

[a]Reaction scale: 0.50–1.0 mmol. [b]The ratio of regioisomers is based on crude NMR after basic work-up. [c]Isolated yield corresponding to the major isomer (indicated as *position A* on arenes). [d]The ratio of regioisomers is based on isolated yields.

For aryl amines **6**–**10** and **16**, the regioselectivity of C–H amination was highly improved. In addition, a smaller number of isomeric products were observed for aniline **13**. However, in the cases of relatively electron-deficient arenes **2**, **11**, and **22**, regioselectivity was not changed noticeably. It was also found that such electron-poor arenes led to lower isolated yield with TFA compared to with TMS-triflate. The experimental data above supports our general interpretation of the calculations that the regioselectivity in arene C–H primary aminations by aminium radical cations is not generally governed by steric effects of the substituents on the nitrogen atom.

Because the result of **TS-1** is a dearomatized carbon radical intermediate, we thought that radical stability would provide an electronic regioselectivity model. Consistent with this initial thinking, the energy landscape in Figure 2 shows that the 3-position **INT-2** (black landscape) is lower in energy than the 5-position **INT-2** (blue landscape). Therefore, we examined if the relative regioisomeric radical stabilities of **INT-2** would provide us with the ability to predict the major products for aryl amines **2**, **6**, **7**, **9**, **12**, **14**, **15**, and **16**. To our surprise, this radical stability analysis of **INT-2** was not general and predicted the major aryl amine products for only half of the arene substrates correctly. Because a radical stability model was not predictive, we wanted to find an alternative, easy to implement analysis that would provide relatively high accuracy in predicting the major primary aniline regioisomer (i.e., the major product). Our goal was not to identify a quantitative model since we do not have experimental kinetic ratios. Therefore, we examined the possibility that regioselectivity of **TS-1** is charge-controlled due to developing partial positive charge within the arene ring as it interacts with $[(TMS)_2NH]^{\bullet+}$ radical cation, as would be expected with an electrophilic aromatic substitution process. We also thought that this charge analysis would be most easily done and highly amplified by analyzing **INT-3**. Figure 3 shows the direct comparison of charged intermediates through analysis of **INT-3**. The

relative energies of **INT-3** provided correct prediction of the major arene products, **6**, **7**, **9**, **12**, **14**, **15**, and **16**. Stated another way, *the more stable cationic **INT-3** maps to the major aryl amine product found experimentally*. Importantly, this type of analysis is related to but fundamentally different from Ritter's use of Fukui functions to analyze the starting arene substrates.[12]

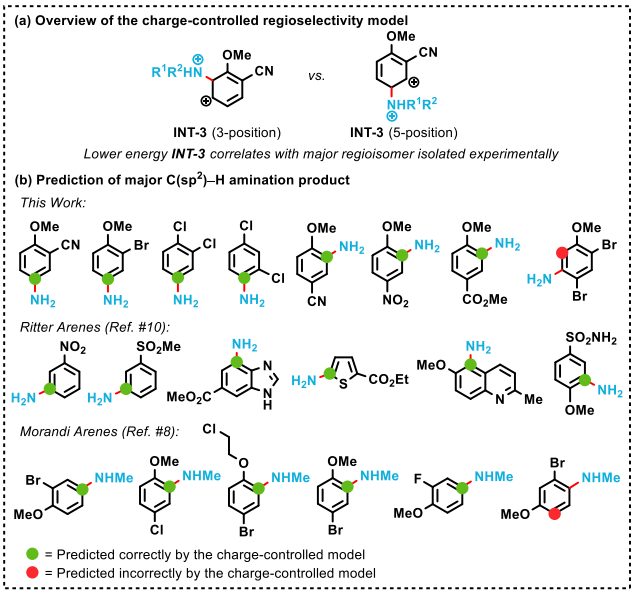

Figure 3. Charge-controlled regioselectivity model and the prediction of major arene C–H amination products using this model.

We wondered if this straightforward comparison of **INT-3** would work to predict the major amination product for arenes beyond the current substrate scope shown in Figure 3. Therefore, we completed this charge analysis using additional 30 arenes found in the reports of Morandi[8] and Ritter.[10] Analysis of the relative positional stabilities for **INT-3** showed that 36/38 arenes correctly predicted the major regioisomer found experimentally (see Figure 3. For the two arenes that this analysis did not work, both had major:minor ratios less than 3.7:1; See SI, Figure 3S for the completed list of the prediction).

CONCLUSIONS

In conclusion, twenty arenes were aminated using MsONHBoc with a single-electron transfer Fe catalyst. Experiments and DFT calculations indicate that contrary to expectations, the regioselectivity of the TMS-substituted aminium radical is not controlled by a steric effect. Rather a relatively general charge-controlled model was identified. This model provides accurate major product prediction for this new set of arene reactants as well as reactions previously reported by Ritter and Morandi.

ASSOCIATED CONTENT

Data Availability Statement

The data underlying this study are available in the published article and its Supporting Information.

Supporting Information

The Supporting Information is available free of charge on the ACS Publications website.

Experimental details, optimization study, compound characterization, NMR spectra, C–H amination with organic acids, and details and supporting data for DFT calculation. (PDF)

Cartesian coordinates (Å). (xyz)

AUTHOR INFORMATION

Corresponding Authors

Daniel H. Ess – Department of Chemistry and Biochemistry, Brigham Young University, Provo, Utah 84602, USA; E-mail: dhe@chem.byu.edu

László Kürti – Department of Chemistry, Rice University, Houston, TX 77030, USA; E-mail: kurti.laszlo@rice.edu

Present Addresses

† **Nicole Erin Behnke** – Janssen Research & Development, San Diego, CA 92121, USA.

Author Contributions

The manuscript was written through contributions of all authors. All authors have given approval to the final version of the manuscript.

‡These authors contributed equally.

Notes

The authors declare no competing financial interest.

ACKNOWLEDGMENTS

This work was supported by Rice University, National Institutes of Health (R35 GM-136373), National Science Foundation (CHE-2102462), and Robert A. Welch Foundation (Grant C-1764). We thank Brigham Young University for computational resources.

REFERENCES

(1) (a) Hili, R.; Yudin, A. K. Making carbon-nitrogen bonds in biological and chemical synthesis. *Nat. Chem. Biol.* **2006**, *2*, 284-287. (b) Roughley, S. D.; Jordan, A. M. The Medicinal Chemist's Toolbox: An Analysis of Reactions used in the Pursuit of Drug Candidates. *J. Med. Chem.* **2011**, *54*, 3451-3479.

(2) (a) Lawrence, S. A. Amines: Synthesis, Properties and Applications; Cambridge University Press, 2004. (b) Rappoport, Z. The Chemistry of Anilines, Parts 1-2; John Wiley & Sons, 2007. (c) Ricci, A. Amino Group Chemistry: From Synthesis to the Life Sciences; Wiley-VCH, 2008. (d) Kürti, L. Streamlining Amine Synthesis. Science **2015**, 348, 863-864.

(3) (a) Kadam, H. K.; Tilve, S. G. Advancement in methodologies for reduction of nitroarenes. *RSC Adv.* **2015**, *5*, 83391-83407. (b) Tafesh, A. M.; Weiguny, J. A Review of the Selective Catalytic Reduction of Aromatic Nitro Compounds into Aromatic Amines, Isocyanates, Carbamates, and Ureas using CO. *Chem. Rev.* **1996**, *96*, 2035-2052. (c) Adams, J. P. Nitro and related groups. *J. Chem. Soc., Perkin Trans. 1.* **2002**, 2586-2597.

(4) (a) Hartwig, J. F. Palladium-Catalyzed Amination of Aryl Halides: Mechanism and Rational Catalyst Design. *Synlett* **1997**, *4*, 329-340. (b) Hartwig, J. F. Carbon-Heteroatom Bond-Forming Reductive Eliminations of Amines, Ethers, and Sulfides. *Acc. Chem. Res.* **1998**, *31*, 852-860. (c) Hartwig, J. F. Transition Metal Catalyzed Synthesis of Arylamines and Aryl Ethers from Aryl Halides and Triflates: Scope and Mechanism. *Angew. Chem. Int. Ed.* **1998**, *37*, 2046-2067. (d) Wolfe, J. P.; Wagaw, S.; Marcoux, J.-F.; Buchwald, S. L. Rational Development of Practical Catalysis for Aromatic Carbon-Nitrogen Bond Formation. *Acc. Chem. Res.* **1998**, *31*, 805-818. (e)

Surry, D. S.; Buchwald, S. L. Biaryl phosphane ligands in palladium-catalyzed amination. *Angew. Chem. Int. Ed.* **2008**, *47*, 6338-6361. (f) Surry, D. S.; Buchwald, S. L. Dialkylbiaryl phosphines in Pd-catalyzed amination: a user's guide. *Chem. Sci.* **2011**, *2*, 27-50. (g) Chan, D. M. T.; Monaco, K. L.; Wang, R.-P.; Winters, M. P. New N- and O-arylations with phenylboronic acids and cupric acetate. *Tetrahedron Lett.* **1998**, *39*, 2933-2936. (h) Evans, D. A.; Katz, J. L.; West, T. R. Synthesis of diaryl ethers through the copper-promoted arylation of phenols with arylboronic acids. An expedient synthesis of thyroxine. *Tetrahedron Lett.* **1998**, *39*, 2937-2940. (i) Lam, P. Y. S.; Clark, C. G.; Saubern, S.; Adams, J.; Winters, M. P.; Chan, D. M. T.; Combs, A. New aryl/heteroaryl C-N bond cross-coupling reactions via arylboronic acid/cupric acetate arylation. *Tetrahedron Lett.* **1998**, *39*, 2941-2944.

(5) (a) Barker, T. J.; Jarvo, E. R. Developments in Transition-Metal-Catalyzed Reactions Using Electrophilic Nitrogen Sources. *Synthesis* **2011**, *24,* 3954-3964. (b) Starkov, P.; Jamison, T. F.; Marek, I. Electrophilic Amination: The Case of Nitrenoids. *Chem. Eur. J.* **2015**, *21*, 5278-5300. (c) Dong, X.; Liu, Q.; Dong, Y.; Liu, H. Transition-Metal-Catalyzed Electrophilic Amination: Application of *O*-Benzoylhydroxylamines in the Construction of the C–N Bond. *Chem. Eur. J.* **2017**, *23*, 2481-2511. (d) Zhou, Z.; Ma, Z.; Behnke, N. E.; Gao, H.; Kürti, L. Non-Deprotonative Primary and Secondary Amination of (Hetero)Arylmetals. *J. Am. Chem. Soc.* **2017**, *139*, 115-118. (e) Gao, H.; Zhou, Z.; Kwon, D.-H.; Coombs, J.; Jones, S.; Behnke, N. E.; Ess, D. H.; Kürti, L. Rapid heteroatom transfer to arylmetals utilizing multifunctional reagent scaffolds. *Nat. Chem.* **2017**, *9*, 681-688. (f) Zhou, Z.; Kürti, L. Electrophilic Amination: An Update. *Synlett* **2019**, *30*, 1525-1535.

(6) (a) Murakami, K.; Perry, G. J. P.; Itami, K. Aromatic C–H amination: a radical approach for adding new functions into biology- and materials-oriented aromatics. *Org. Biomol. Chem.* **2017**, *15*, 6071-6075. (b) Jiao, J.; Murakami, K.; Itami, K. Catalytic Methods for Aromatic C–H Amination: An Ideal Strategy for Nitrogen-Based Functional Molecules. *ACS Catal.* **2016**, *6*, 610-633. (c) Park, Y.; Kim, Y.; Chang, S. Transition Metal-Catalyzed C–H Amination: Scope, Mechanism, and Applications. *Chem. Rev.* **2017**, *117*, 9247-9301. (d) Svejstrup, T. D.; Ruffoni, A.; Juliá, F.; Aubert, V. M.; Leonori, D. Synthesis of Arylamines via Aminium Radicals. *Agnew. Chem. Int. Ed.* **2017**, *56*, 14948-14952. (e) Rössler, S. L.; Jelier, B. J.; Tripet, P. F.; Shemet, A.; Jeschke, G.; Togni, A.; Carreira, E. M. Pyridyl Radical Cation for C–H Amination of Arenes. *Angew. Chem. Int. Ed.* **2019**, *58*, 526-531. (f) Ruffoni, A.; Juliá, F.; Svejstrup, T. D.; McMillan, A. J.; Douglas, J. J.; Leonori, D. Practical and regioselective amination of arenes using alkyl amines. *Nat. Chem.* **2019**, *11*, 426-433. (g) Munnuri, S.; Anugu, R. R.; Falck, J. R. Cu(II)-Mediated N–H and N-Alkyl Aryl Amination and Olefin Aziridination. *Org. Lett.* **2019**, *21*, 1926-1929. (h) See, Y. Y.; Sanford, M. S. C–H Amination of Arenes with Hydroxylamine. *Org. Lett.* **2020**, 22, 2931-2934. (i) Wang, T.; Hoffmann, M.; Dreuw, A.; Hasagić, E.; Hu, C.; Stein, P. M.; Witzel, S.; Shi, H.; Yang, Y.; Rudolph, M.; Stuck, F.; Rominger, F.; Kerscher, M.; Comba, P.; Hashmi, A. S. K. A Metal-Free Direct Arene C–H Amination. *Adv. Synth. Catal.* **2021**, *363*, 2783-2795.

(7) Paudyal, M. P.; Adebesin, A. M.; Burt, S. R.; Ess, D. H.; Ma, Z.; Kürti, L.; Falck, J. R. Dirhodium-catalyzed C–H arene amination using hydroxylamines. *Science* **2016**, *353*, 1144-1147.

(8) Falk, E.; Gasser, V. C. M.; Morandi, B. Synthesis of *N*-Alkyl Anilines from Arenes via Iron-Promoted Aromatic C–H Amination. *Org. Lett.* **2021**, *23*, 1422-1426.

(9) Legnani, L.; Cerai, G. P.; Morandi, B. Direct and Practical Synthesis of Primary Anilines through Iron-Catalyzed C–H Bond Amination. *ACS Catal.* **2016**, *6*, 8162-8165.

(10) D'Amato, E. M.; Börgel, J.; Ritter, T. Aromatic C–H Amination in Hexofluorosiopropanol. *Chem. Sci.* **2019**, *10*, 2424-2428.

(11) Liu, J.; Wu, K.; Shen, T.; Liang, Y.; Zou, M.; Zhu, Y.; Li, X.; Li, X.; Jiao, N. Fe-Catalyzed Amination of (Hetero)Arenes with a Redox-Active Aminating Reagent under Mild Conditions. *Chem. Eur. J.* **2017**, *23*, 563-567.

(12) Boursalian, G. B.; Ham, W. S.; Mazzotti, A. R.; Ritter, T. Charge-transfer-directed radical substitution enables *para*-selective C–H functionalization. *Nat. Chem.* **2016**, *8*, 810-815.